

We are IntechOpen, the world's leading publisher of Open Access books Built by scientists, for scientists

4,800

Open access books available

122,000

International authors and editors

135M

Downloads

Our authors are among the

154

Countries delivered to

TOP 1%

most cited scientists

12.2%

Contributors from top 500 universities



WEB OF SCIENCE™

Selection of our books indexed in the Book Citation Index
in Web of Science™ Core Collection (BKCI)

Interested in publishing with us?
Contact book.department@intechopen.com

Numbers displayed above are based on latest data collected.
For more information visit www.intechopen.com



Welding and Joining of Magnesium Alloys

Frank Czerwinski
Bolton, Ontario
Canada

1. Introduction

Welding and joining of magnesium alloys exert a profound effect on magnesium application expansion, especially in ground and air transportations where large-size, complex components are required. This applies to joints between different grades of cast and wrought magnesium alloys and to dissimilar joints with other materials, most frequently with aluminum and steel.

Due to specific physical properties of magnesium, its welding requires low and well controlled power input. Moreover, very high affinity of magnesium alloys to oxygen requires shielding gases which protect the liquid weld from an environment. To magnify complexity, also solid state reaction with oxygen, which forms a thermodynamically stable natural oxide layer on magnesium surface, is an inherent deficiency of joining (Czerwinski, 2008). Both the conventional and novel welding techniques were adapted to satisfy these requirements, including arc welding, resistance spot welding, electromagnetic welding, friction stir welding, electron beam and laser welding. Since fusion welding has a tendency to generate porosities and part distortion, many alternative joining practices were implemented. These include soldering, brazing, adhesive bonding and mechanical fastening. However, also the latter techniques have disadvantages associated, for example, with stress induced by drilling holes during mechanical fastening, preheating during clinching or extensive surface preparation in adhesive bonding. Hence, experiments are in progress with completely novel ideas of magnesium joining.

An application of magnesium is often in multi-material structures, requiring dissimilar joints, involving magnesium alloys as one side where on another end there are alloys with drastically different properties. How to weld dissimilar materials is one of the most difficult problems in welding. A difference in physicochemical properties of dissimilar joint components creates challenges for mechanically bolted assemblies as well. Due to its very low electronegative potential, magnesium is susceptible to galvanic corrosion thus affecting performance of mechanical joints in conductive environments.

This chapter covers key aspects of magnesium welding and joining along with engineering applications, challenges and still existing limitations. For each technique, the typical joint characteristics and possible defects are outlined with particular attention paid to weld metallurgy and its relationship with weld strength, ductility and corrosion resistance. Although fundamentals for each technique are provided, the primary focus is on recent global activities.

2. Arc welding

There are two basic methods of arc welding. In an inert gas tungsten arc welding (TIG), an arc is generated between a non-consumable tungsten electrode and the welded metal. The electrode and welded metal are shielded with an inert gas, typically argon. In general, weld can be made with or without filler. In case the filler is used, it has a form of wire, provided to the weld. For magnesium alloys, filler rods may be of the same chemistry as welded part or lower melting range. The latter allows the weld to remain liquid until other parts of the weld are solid, thus reducing the probability of cracking. During an inert gas metal arc welding (MIG), the arc is formed between the consumable electrode and the part to be welded. The electrode is continuously provided from the spool. Both the welded area and the arc zone are protected by a gas shield.

The specific heat of magnesium is around $1 \text{ J g}^{-1} \text{ } ^\circ\text{C}^{-1}$ but due to lower density of magnesium, its heat capacity is lower than aluminum or steel (Table 1). Due to similar melting ranges of Mg and Al alloys and the lower latent heat of fusion of magnesium alloys the heat required to melt magnesium is two third of that required for melting the same volume of aluminum alloys. Relatively high coefficient of thermal expansion of magnesium alloys of $26 \mu\text{m m}^{-1} \text{ } ^\circ\text{C}^{-1}$ and high thermal conductivity of $51 \text{ Wm}^{-1}\text{K}^{-1}$ make it susceptible to distortion during welding.

Property	Units	AZ91	A6061	ZA12	Steel 304
Melting range	$^\circ\text{C}$	470-595	582-652	377-432	1400-1455
Density	g cm^{-3}	1.8	2.7	6.0	8.0
Modulus of elasticity	GPa	45	68.9	83	200
Thermal conductivity (20 $^\circ\text{C}$)	$\text{Wm}^{-1}\text{K}^{-1}$	51	180	116	16.2
Coefficient of thermal expansion (20-100 $^\circ\text{C}$)	$\mu\text{m m}^{-1} \text{ } ^\circ\text{C}^{-1}$	26.0	23.6	24.1	17.2
Specific heat (20 $^\circ\text{C}$)	$\text{J g}^{-1} \text{ } ^\circ\text{C}^{-1}$	0.8	0.896	0.450	0.5
Latent heat of fusion pure base metals	J/g	368	398	272	113
Electrical resistivity	$\mu\Omega\text{m}$	0.0000143	0.00000360	0.00000610	0.0000720

Table 1. Selected properties of AZ91 magnesium alloy, A6061 aluminum alloy, ZA12 zinc alloy and AISI 304 stainless steel (Avedesian, 1999), (ASM, 1990)

For transition metal alloys, a technique exists of flux-assisted gas tungsten arc welding (FA-TIG) when the welding path is coated with chemical fluxes. In general, fluxes allow full penetration welding at greater rates using relatively inexpensive gas tungsten arc as the heat source. Using argon shielding and chloride fluxes, magnesium alloy welding tests showed an increase in weld penetration as much as one hundred percent (Marya and Edwards, 2002). The deeper weld penetration was accompanied by higher heat input. Among several chlorides, including LiCl , CaCl_2 , CdCl_2 , PbCl_2 and CeCl_3 , cadmium chloride was the most effective. Images of arc area during welding revealed that the heat flux from the arc appeared more concentrated towards the center of the pool with chloride additions.

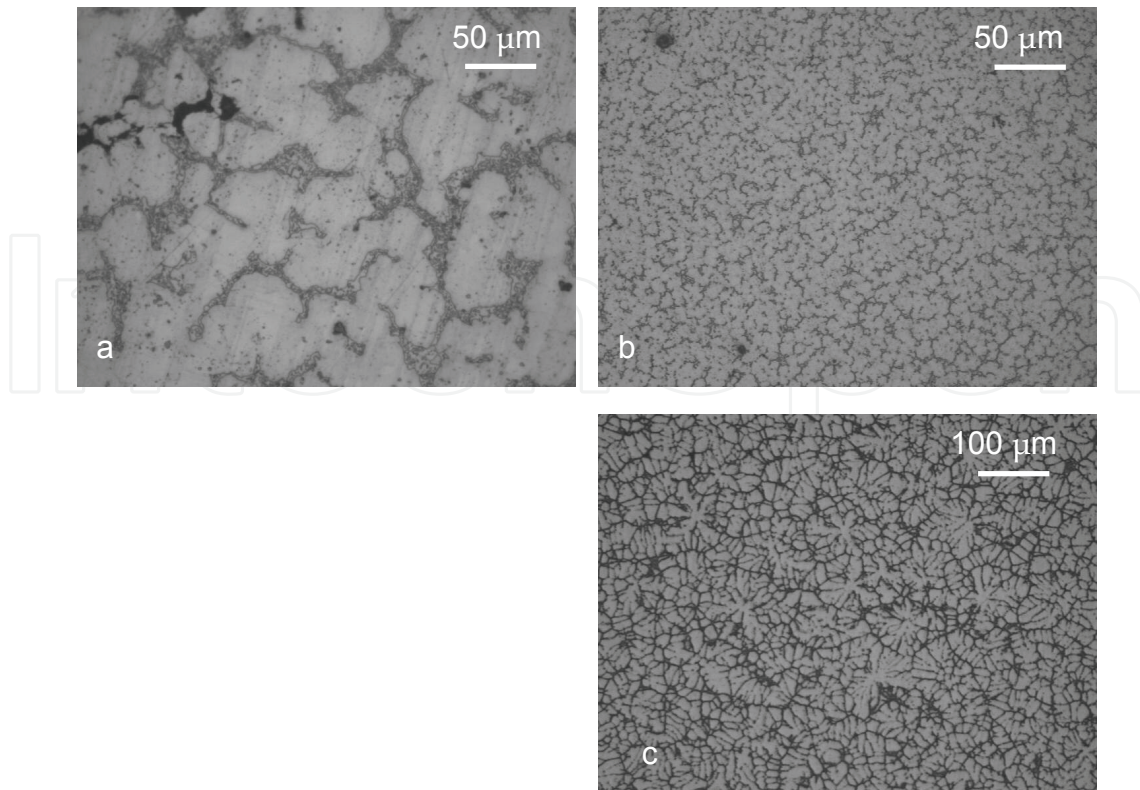


Fig. 1. Effect of cooling rate during solidification on microstructure of magnesium and aluminum alloys: (a) AZ91 slow cooling; (b) AZ91 rapid cooling; (c) A356 rapid cooling.

2.1 Weld microstructure

The solidification microstructure of the weld is controlled by constitutional undercooling, depending on the thermal gradient and growth rate (Fig. 1). The microstructure of MIG welded AZ91D alloy with AZ61 as welding wire consisted of solid solution of α -Mg and intermetallic compound of $Mg_{17}Al_{12}$ (Sun et al., 2008). The weld contained roughly 7% of Al. In HAZ near the fusion line, subjected to temperatures between solidus and liquidus, a part of α -Mg solid solution and eutectics, distributed at grain boundaries, experienced melting. Thus, after subsequent solidification the boundary regions formed islands of eutectic solid solution of α -Mg surrounded by $Mg_{17}Al_{12}$ precipitates. The chloride fluxes during welding using FA-TIG technique affected the weld microstructure (Marya and Edwards, 2002). It appears that alloying from fluxes did not drastically affect the solute partitioning during solidification. The AZ21 fusion zone, obtained with cadmium chloride fluxes, was significantly more dendritic than the zone of the alloy identically welded without fluxes. It is believed that differences in microstructure between welds with and without chloride fluxes are caused by thermal gradient. During welding with cadmium chloride, the arc temperature was significantly higher and the liquid weld experienced higher constitutional undercooling.

2.2 Weld cracking

In addition to extensive porosity, as shown in Fig. 2, hot cracking is considered the major problem of magnesium welding. This is especially true for a repair practice where thick plates are welded using the metal inert gas technique. During MIG welding of 10 mm thick

plates of AZ91D, two types of hot cracking occurred: solidification cracking of weld and liquation cracking in HAZ (Sun, et al., 2008). In general, solidification cracking takes place within a specific temperature range when a liquid film appears between dendrites. Solidification cracking occurred within the crater at the weld end and was caused by the high segregation of Mn, Al and Zn accompanied by high tensile stress. A frequency of both types of cracks increased at low welding speeds and was associated with high heat input and tensile stress. The experimental observations indicate that for MIG welding of magnesium alloys a reduction in the heat input reduces the frequency of cracks in weld and HAZ.

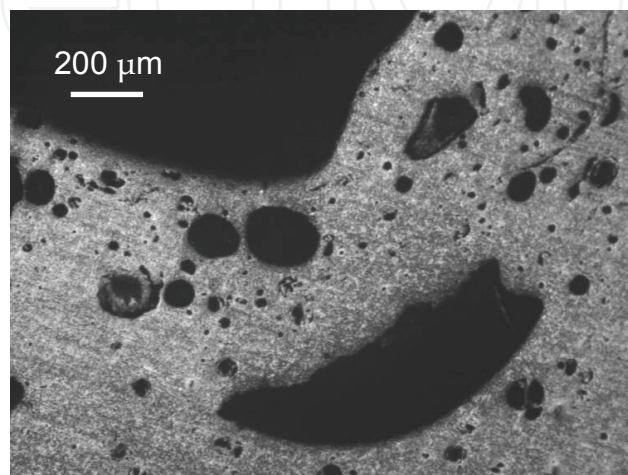


Fig. 2. Gas porosity in a weld of magnesium alloy Mg-8%Al.

3. Laser beam welding

The term laser is an acronym for “Light Amplification by Stimulated Emission of Radiation”. The solid or gaseous media are stimulated to emit a monochromatic, coherent source of light which is then focused to a point source and delivered to the workplace. A delivery by hard optics explores mirrors and lenses for laser deflection and focusing. A limitation of hard optics is the short distance between the laser source and welded part. The use of fiber optics cable allows for a longer separation of laser source. The latter is also more suitable for manipulation by robotics. There are two major types of lasers, commonly used in industrial applications. The laser of Nd:YAD – Neodymium-doped Yttrium-Aluminum-Garnet explores a crystalline rod and emits light in the ultraviolet range with a wavelength of 1.06 μm . The CO₂ laser is based on gaseous media and has a wavelength of 10.6 μm .

3.1 Process and its advantages

During welding the laser fires many pulses per second (Fig. 3). The light is absorbed by the metal, causing the “keyhole” effect since the beam drills, melts and vaporizes some metal volume. When the pulse ends, the molten metal around the “keyhole” flows back, and after solidification forms a spot weld. A shielding gas is used to protect the molten metal. Welds may be created with a filler metal or without it. As major benefits of laser beam welding there are quoted: high travel speeds, minimal amount of heat added during welding, resulting in a small heat affected zone, low part distortion, no slag or spatter and great flexibility in tooling design.

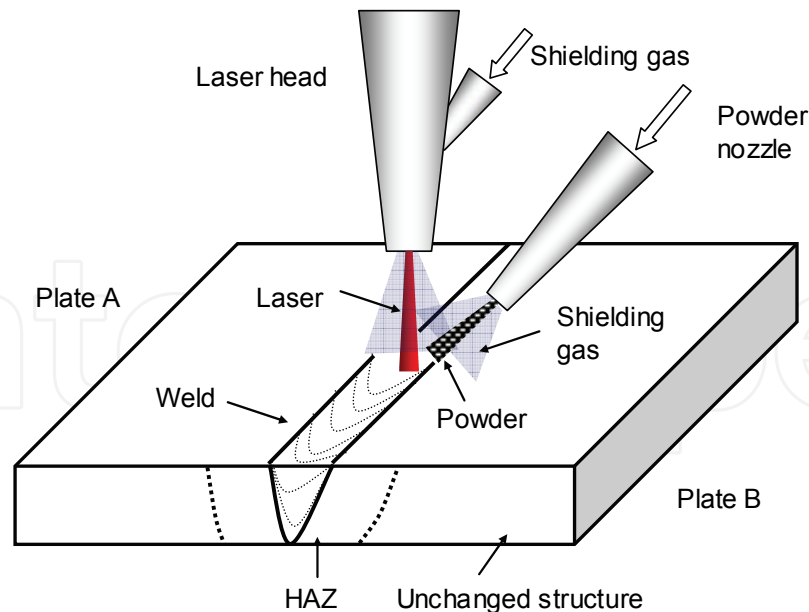


Fig. 3. Schematic of laser beam welding process

3.2 Weld structure, defects, process modeling

The AM60 alloy, welded with a continuous wave CO₂ laser, formed a weld with the narrow heat affected zone and no obvious grain coarsening (Quan et al., 2008). The fusion zone was fine-grained with high density of Mg₁₇Al₁₂ precipitates. The redistribution of elements occurred during welding with lower Mg and higher Al content in weld than in the base alloy. A hardness of the fusion zone reached the higher level than of the base alloy.

The mechanism of porosity formation during continuous-wave Nd-YAG laser beam welding of AM60B cast alloy revealed a significant increase in fusion-zone porosity for most of welding conditions (Zhao and DebRoy, 2001). The pre-existing pores, their coalescence and expansion were seen as the cause of porosity increase. The keyhole was found more stable than during welding of Al alloys but its stability did not substantially affect the overall porosity. During CO₂ laser welding of AZ31 wrought alloy, pores were found in welds mainly around the fusion boundary (Zhou et al., 2005). Since in wrought alloy the level of initial porosity is relatively low, pore formation during welding is attributed to the surface contamination and hydrogen rejection from the solid phase during solidification. It appears that porosity is created due to a collapse of the keyhole and turbulent flow in the weld. An example of welding speed effect on porosity is shown in Fig. 4.

In recent attempt, an analytical thermal model for welding the magnesium alloy WE43 was developed (Abderrazak et al., 2008). Since laser welding is controlled by many parameters including power, beam characteristics, welding speed, focal position, gas flow and material characteristics, finding the optimum is a complex task. The model allows determining the penetration depth and the bead width as a function of both the incident laser power and the welding speed. Modeling along with experimental verification were also used to study the keyhole formation and the geometry of weld profiles during welding of ZE41A-T5 alloy with Nd-YAG laser (Al-Kazzaz et al., 2008). Generally, the weld width and fusion area decrease with increasing welding speed. It was found that the excessive reduction in laser power resulted in lower surface power density and change of the welding mode through partially penetrated keyhole to the conduction mode. There was no significant effect of the filler wire feed rate on the coupling and melting efficiency.

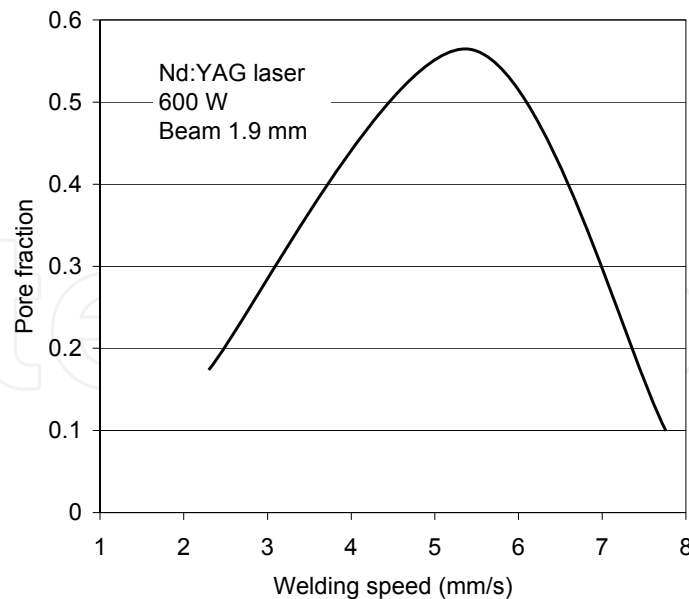


Fig. 4. Effect of welding speed on the pore fraction in AZ91 alloy weld (Marya and Edwards, 2000)

3.3 Hybrid laser beam welding

Hybrid laser beam technologies are defined as a combination of a laser beam source with an additional secondary beam source or another joining technique. A hybrid laser-TIG welding (LATIG) of AZ31 alloy, achieved higher welding speed than in laser or TIG welding (Liu et al., 2004). The penetration depth was twice of that for TIG and four times of that for laser welding. The same combination of laser beam and TIG was used to weld AZ31B magnesium alloy with a mild steel, applying a nickel interlayer (Qui and Song, 2010). As a result, semi-metallurgical bonding was achieved. Along the Mg - Ni interlayer the Mg_2Ni phase with solid solution of Ni in Fe formed. However, at the interface of molten pool and steel, the fusion zone did not interact with solid solution, suggesting mechanical bonding.

A new method of hybrid joining, called laser continuous weld bonding, was developed as an alternative to laser welding and adhesive bonding (Liu et al., 2007a). The technique was successful in joining of AZ31B magnesium and A6061 aluminum alloys by reducing a volume of brittle intermetallic compounds of Al_3Mg_2 and $Mg_{17}Al_{12}$ phases which are formed in the fusion zone, reducing the joint strength. The intermetallic phase formation was reduced due to the fluid generated by the gasification of adhesives. It appears that rising of adhesive vapor slows down the downward movement of liquid Mg, thus reducing its content in the weld. Hence, the weld is composed of two-phase mixture with less intermetallic compound and more solid solution.

4. Resistance spot welding

Resistance spot welding represents the localized joining of two or more metal parts together by an application of heat and pressure. The weld is formed due to the heat generated by the resistance to the electrical current passage between copper electrodes, being also the source of pressure. As a result, at the interface of welded materials a liquid pool (weld nugget) is formed. For high electrical conductivity of magnesium and low heat generation in the weld,

high welding currents are required. The process is used mainly in assembly lines to weld products made of thin gauge metals and it has potentials for joining sheets of magnesium alloys.

4.1 Weld microstructure

The joint obtained with a technique of resistance spot welding consists of the weld nugget and the heat affected zone. For AZ31 alloy the weld nugget contained the cellular dendritic structure at nugget edge, accompanied by equiaxed dendritic structure within its center (Sun et al., 2007). The boundary melting and coarsening was observed in the heat affected zone. It was revealed that the weld nuggets show a tendency to hot cracking. The joint strength and cracking susceptibility are influenced by the welding current. While the higher current increases strength it also increases the nugget tendency to cracking.

4.2 Effect of welding parameters on joint properties

The influence of selected process parameters on joint properties is shown in Fig. 5 (Shi, et al., 2010). For a constant electrode force, an increase in current reduces weld integrity as seen through porosity level (Fig. 5, left). An increase in the electrode force reduces the role of current and at sufficiently high electrode force the effect of current disappears. To improve heat generation at the connection, cover plates made of cold rolled steel were implemented. The plates allowed obtaining joints with larger weld nuggets and higher strength by applying the reduced current. As was the case without steel plates, the reduction in pore formation was achieved by increasing the electrode force and extending the holding time after current shut-off. The relative importance of holding time after current shut-off depended on welding current.

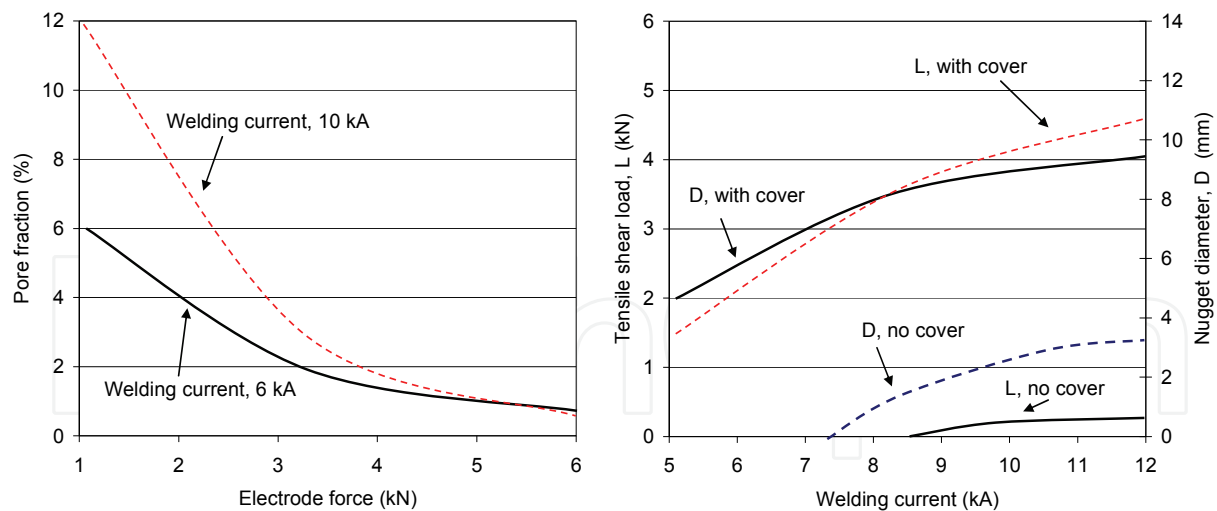


Fig. 5. Resistance spot welding of AZ31B alloy without and with steel cover plates: (left) pore fraction versus electrode force; (right) tensile shear load and nugget diameter as a function of welding current (Shi et al., 2010)

5. Friction stir welding

Friction stir welding is a relatively new joining technique and was invented in 1991 by The Welding Institute, England (TWI). It uses a rotating, non-consumable, cylindrical-

shouldered tool to deform the surrounding material without melting. Thus, the joint is essentially formed in a solid state. The concept is depicted in Fig. 6. Due to frictional contact of the tool and welded parts the heat generated plasticizes metal. As the tool moves forward, its special profile forces the plasticized material to the back and due to substantial forging force consolidates material so the joint is formed. The process is accompanied by severe plastic deformation, involving dynamic recrystallization of the base metal (Kumbhar and Bhanumurthy, 2008).

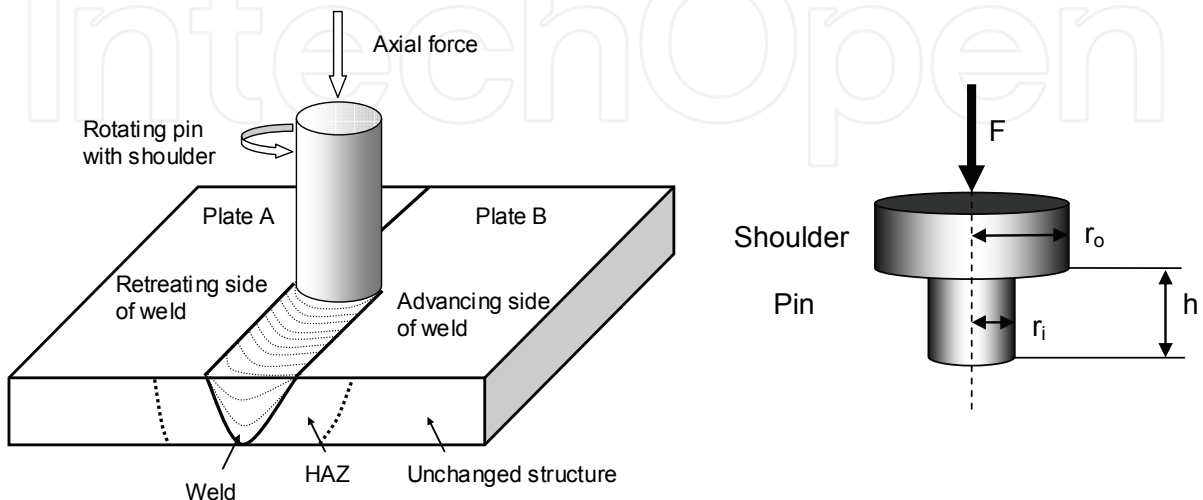


Fig. 6. Schematics of friction stir welding process and tool geometry

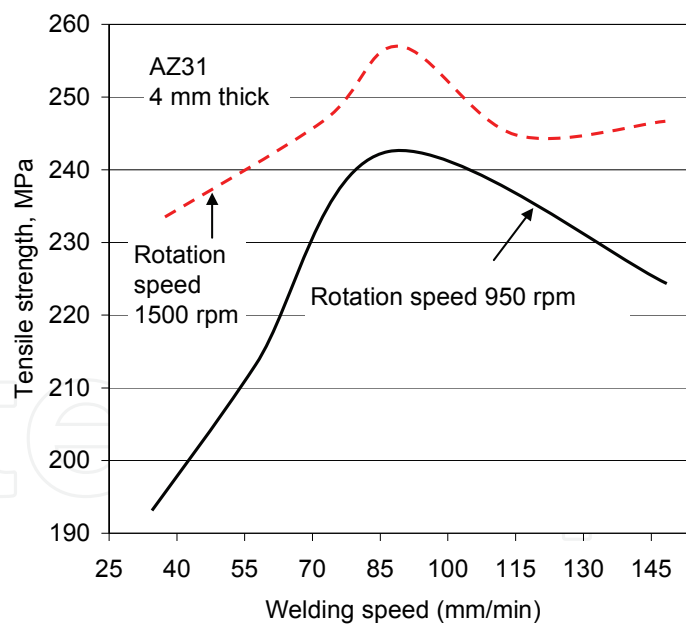


Fig. 7. Influence of welding speed and rotation speed on tensile strength of friction stir weld of AZ31 magnesium alloy plates with a thickness of 4 mm. The tool pin diameter is 4 mm and the shoulder diameter is 12 mm (Wang and Wang, 2006)

The total energy generated per unit length of the weld E equals the energy due to friction between the tool and the work piece E_f and the energy generated due to the plastic deformation of the work piece E_p (Emam and Domiaty, 2009):

$$E = E_f + sE_p \quad (1)$$

where: s is the scaling factor introduced in order to control the effect of the energy due to plastic deformation. The friction component E_f is expressed by:

$$E_f = 2\mu F \left(\frac{1}{3}r_o + \frac{r_i^2}{r_o^2}h \right) \frac{\omega}{v_o} \quad (2)$$

Where: r_o is the radius of the shoulder, r_i is the radius of the pin, h is the height of the pin (Fig. 6), ω is the pin angular speed, μ is the friction coefficient, F is the compressive force. The component E_p , associated with the plastic deformation, is defined as follows:

$$E_p = K\varepsilon^{n+1} (2r_i h) \exp\left(\frac{mQ}{R_G T}\right) \quad (3)$$

where: K is the strength coefficient, n is the strain hardening exponent, m is the strain rate sensitivity, Q is the apparent activation energy, R_G is a constant equals $8.32 \text{ J}^{-1}\text{K}^{-1}$, T is the absolute temperature. The heat due to the plastic deformation has a significant effect on final temperature, especially at low energy levels.

There are many benefits associated with friction stir welding. A low heat input and bonding below the melting point result in higher joint properties and lower distortion. The severe plastic deformation, introduced by the tool action, generates the fine-grained microstructure. The process is energy efficient and environmentally friendly with no fumes or UV radiation. Since there is no weld gravity issue, various welding positions are possible as orbital, vertical or overhead. As likely drawbacks of friction stir welding the large force and system stiffness requirements are quoted. Another drawback was a fixed pin capable handling of only one material thickness. However, modern solutions offer pins which can retract or expand within material thus allowing welding components with varying thickness.

5.1 Application to magnesium joints

Friction stir welding is extensively applied for magnesium alloys and for dissimilar joints with a magnesium component (Fig. 7).

The development of weld microstructure is controlled by shear deformation and thermal effects. In weld of wrought AZ61 alloy the crystallographic texture develops with a strong concentration of {0001} basal planes, being heterogeneously distributed in stir zone (Park et al., 2003). It was suggested that texture develops due to shear deformation caused by the rotating pin. Deformation of magnesium with hexagonal close packed structure is controlled by a slip along {0001} basal plane. Therefore, formation of this type of texture during welding affects the mechanical properties of weld. During friction stir welding of two AZ61 plates with a thickness of 6.3 mm both the transition and stir regions developed similar grain size, much finer than in the base alloy (Park et al., 2003a).

The technique of friction stir welding was applied to join magnesium with steel. During welding of AZ31 alloy and stainless steel 400, the rotation speed and pin axis orientation affected the microstructure and strength of the joint (Watanabe et al., 2006). The maximum strength of a butt type joint achieved approximately 70% of the strength measured for pure magnesium. The effect of tool geometry on microstructure and mechanical properties of Mg-steel welding was also studied (Chen and Nakata, 2009). For brushed finished steel joints,

the strength increased significantly with the probe length. Also microstructure was found to be sensitive to the probe length. The longer probe resulted in diffusion bonding while the shorter probe provided only the mechanical bond. The different observations were recorded for zinc coated steel where the probe length did not improve the joint strength. In that case, the short probe contributed to the defect-free joint.

Alloy	Weld/parent	Tensile strength, MPa	Yield stress, MPa	Elongation, %	Literature
AZ31	weld	201	125	3.7	1
	parent	255	200	12	2
AZ91	weld	183	153	1.5	1
	parent	250	160	3	2
	weld	200	150	2	4
AZ61	weld	280	120	17	3
	parent	310	230	25	2
AM50	weld	164	110	4	1
	parent	230	125	15	2
	weld	150	100	3	4

Table 2. A comparison of tensile properties of selected magnesium alloys after friction stir welding with properties of parent alloys. References: (1) (Johnson and Threadgill, 2003); (2)(Avedesian, 1999); (3) (Park, et al., 2003a); (4) (Skar et al., 2004)

6. Electromagnetic welding

Electromagnetic welding explores a phenomenon that current carrying conductors exert a force on each other (Fig. 8). The force depends on the current direction and is repulsive for opposite direction flow and attractive for the same flow direction. In practice, the electric current in the coil creates an eddy current within the work piece which generates forces between the coil and the material placed within it. During the welding process, these forces cause the outer work piece to plastically deform after it accelerates towards the inner work piece, thus creating a solid state weld. There are several modifications of magnetic welding which were successfully applied for magnesium. Similar concept of electromagnetic compression forming was used for processing of hollow profiles of magnesium alloys (Psyk et al., 2006).

Magnetic pulse welding is a solid state joining process and has a modification called pressure seam welding (Lee et al., 2007). Very high currents are generated by discharging a set of charged capacitors rapidly through the coil which surrounds the component to be welded. The eddy currents oppose the magnetic field in the coil and a repulsive force is created which drives the parts together at very high force speed and creates an explosive or impact type of weld. The eddy current i is expressed by the following equation (Aizawa et al., 2007):

$$\nabla \times i = -\kappa \left(\frac{\partial B}{\partial t} \right) \quad (4)$$

where: κ and B are electrical conductivity and magnetic flux density, respectively.

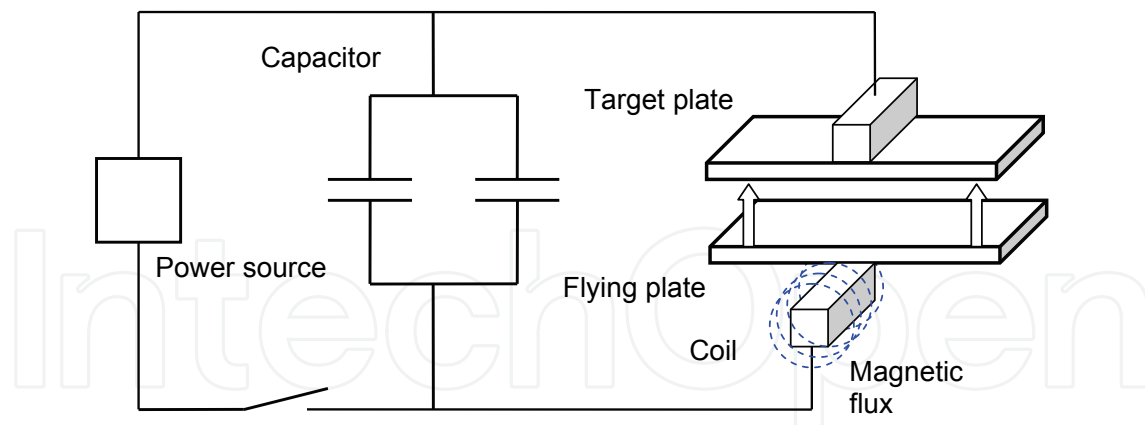


Fig. 8. Schematic diagram of electromagnetic pulse welding

The magnetic pressure p generated is given as follows:

$$p = (B_o^2 - B_i^2) / 2\mu = \left(\frac{B_o^2}{2\mu} \right) (1 - e^{-2x/\delta}) \quad (5)$$

Where: B_o^2 and B_i^2 are magnetic flux densities at lower and upper surfaces of welded sheet, μ is magnetic permeability, δ is the depth skin effect, given by the following:

$$\delta = \sqrt{2 / \omega \kappa \mu} \quad (6)$$

Where: ω is the angular frequency of changing field.

The technique provided satisfactory results for Al- AZ91 magnesium alloy. The sheets with a thickness of 0.5 to 1 mm were seam welded, producing a weld having the width of 5 mm. The weld thickness was 10% less than the original sheet thickness (Aizawa and Kashani, 2010). It is believed that the weld zone is formed as a combined effect of heating by eddy currents and the strong impulse electromagnetic force (magnetic pressure). No clear fusion boundary in the joint interface was microscopically detected. The transition layer had the characteristic wavy shape without any significant heat affected zone.

The same concept, called electromagnetic impact welding, was used for 0.6 mm sheet of AZ31 magnesium alloy and 1 mm thick A3003 aluminum alloy (Kore et al., 2009). The difference in electrical conductivities of Al and Mg led to the skin depth of 0.7 mm in Al and 0.6 mm in Mg alloys. The weld microscopy revealed a wavy interface and complete metal continuity without weld defects. Both x-ray diffraction and electron microscopy did not detect the intermetallic phase at the interface, suggesting a lack of melting. When welding was conducted at optimum conditions, failure during tensile testing occurred beyond the weld, in the base metal.

The electromagnetic compression of tubular profiles with high electrical conductivity is an innovative joining process for lightweight materials. The components are joined using pulsed magnetic fields which apply radial pressures of up to 200 MPa to the material causing a symmetric reduction of the diameter with typical strain of about 10^{-4} s^{-1} (Barreiro et al., 2008). Since there is no contact between components to be joined and the joining machine, there is not possible damage of the welded parts. The method was tested for aluminum alloys and has potentials for magnesium.

7. Electron beam welding

Electron beam welding (EBW) is a fusion welding which employs a dense stream of high velocity electrons to bombard, heat and melt the materials being joined. The electron beam is generated by electron gun composed of a cathode made of tungsten and an anode placed in high-vacuum. When the electron beam moves forward, the melted and evaporated alloy flows from the front to the back of the keyhole. It was developed in 1950's and first applied in nuclear industry. It is suitable for difficult welding where high repeatability is required. When compared to arc welding, EBW creates the narrower weld and heat affected zone. The present drawbacks include high equipment cost, work piece size limitations, or X-ray generation during the electron bombardment.

During 3-dimensional modeling of thermal effect during welding of AZ61 alloy it was found that the welding heat source of electron beam produces two special thermal effects: deep-penetration thermal effect and surface thermal effect of metal vapor (Luo et al., 2010a). The experimental data for AZ61 alloy showed that the key parameters affecting the keyhole thermal effect are the welding heat input and focus coil current, which has also an impact on the weld shape.

A range of welding parameters of electron beam welding was analyzed to assess their importance on weld quality of AZ-series of magnesium alloys (Chi et al., 2008). The following ranking, in order of decreasing influence, was established: beam oscillation, focal position, stress relief, material difference, beam current, welding speed, and accelerating voltage. The best choices were a non-oscillating beam, a focus at the bottom and no stress relief. Of a number of alloys tested, the weldability, as determined by defects and precipitates distribution, follows the order of AZ61, AZ91, and AZ31 with AZ61 being the best.

During electron beam welding of 11 mm thick AZ31B plates with a power of 3000 W to 5000 W the effect of various process parameters was examined (Chi and Chao, 2007). The factors reducing the weld strength were: deviations of weld geometry, porosity and grain coarsening. In general, the weld strength reached over 90% of that for the base alloy.

8. Diffusion bonding

Diffusion bonding represents a solid state joining, achieved where two materials are brought into close contact at elevated temperatures of less than $0.7 T_m$ under moderate pressure, thus the atomic migration is not accompanied by macro-deformation. Since temperature does not exceed melting, it allows to eliminate many problems associated with fusion welding. The process is typically conducted in a press, heated by conventional methods or induction units. Microwave sources are also explored for this purpose. To obtain high bonding, the surface should be clean and flat. There are three major stages of the bonding progress. First, a contact between materials occurs through the mating surfaces (Poddar, 2009). During the second stage, diffusion within grain boundaries predominates, thus eliminating pores and ensuring arrangements of grain boundaries. During the third stage, the volume diffusion dominates and process is completed.

8.1 Joints between magnesium alloys

Diffusion bonding was found applicable for pure magnesium and its alloys. For pure magnesium rolled sheet, tests were carried out at the pressure range of 2-20 MPa, temperature range from 300 °C to 400 °C and time periods up to 72 h (Somekawa et al.,

2001). The maximum lap shear strength was 0.888 at a bonding pressure of 20 MPa, temperature 400 °C and for time of 1 h. A ductile fracture was revealed after the compression lap shear test.

During manufacturing of complex sheet structures, diffusion bonding is often combined with superplastic forming. The combination allows to reduce weight and fabrication cost, as compared with mechanically fastened structures (Gilmore et al., 1991). The technology was successfully implemented for superplastic magnesium alloy AZ31 with a grain size of approximately 17 μm (Fig. 9) (Somekawa, et al., 2003a). The maximum of lap shear strength was 0.85 at a bonding pressure of 3 MPa and a bonding temperature of 400 °C and time of 3 h. No bond line was revealed during microscopic observations, indicating the extensive diffusion. A successful diffusion bonding was also achieved for a superplastic alloy AZ31 hot rolled at 250 °C (Somekawa et al., 2003b). Having a grain size of 8.5 μm , the alloy behaved in a superplastic manner within the temperature range of 250-300 °C. Both phenomena, the diffusion bonding and superplasticity are grain size dependant, thus structures with finer grains will have lower bonding temperature. The effect is related to the bonding mechanism where diffusion controls the joint formation. The numerous voids, initially present at the interface between joined metals will disappear due to the plastic flow and diffusion towards the void surface. For finer grains the boundary diffusion has the higher contribution because more grain boundaries intersect with voids.

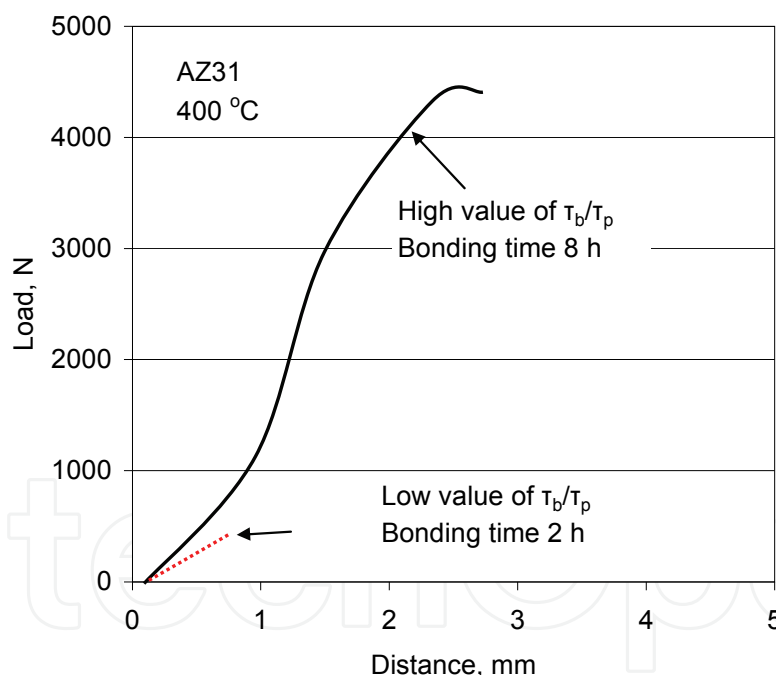


Fig. 9. Load versus distance measured during the compression lap test of diffusion bonded AZ31 magnesium alloy (Somekawa et al., 2003a)

8.2 Dissimilar joints formed by diffusion bonding

For dissimilar joints of Mg alloys, of special importance is Al. This is due to the substitution of Al with Mg in automotive industry, which requires Mg-Al joints. An example is the Mg/Al joint made using vacuum bonding at 460-480 °C, time of 40-60 min and a pressure of 0.08-0.10 MPa (Li et al., 2008). Hence, the diffusion zone was formed with two different transition regions on both sides. At the interface with Al, various Mg_xAl_y phases, such as

MgAl, Mg₃Al₂ and Mg₂Al₃ were formed. On the Mg side in addition to Mg grains, Mg₃Al₂ phase was formed. The latter has fcc structure as opposed to hcp of magnesium. It is claimed that Mg₃Al₂ phase has the positive effect on cracking resistance of the joint.

The major obstacle during welding of Mg and Al is a formation at the interface between both alloys brittle compounds of Mg-Al, causing cracking during service. Thus eliminating or improving that interlayer is the critical factor in producing strong joints. One of possible solutions is to introduce an interlayer between Al and Mg. For AZ31B and A6061 alloys, Zn interlayer was found to be effective (Zhao and Zhang, 2008). The Zn layer with a thickness of 60 µm was deposited on Al surface by hot dipping. The bonding was conducted at 360 °C for 3 s.

Diffusion bonding was proved effective for joining Mg with alloys having substantially higher melting ranges, such as Cu alloys. Joints made at the bonding temperature of 450 °C, pressure of 12 MPa and time of 30 min exhibited shear strength of 66 MPa and bonding strength of 81 MPa (Mahendran et al., 2010).

8.3 Experimental joining techniques

The new technique of in-situ joint formation of magnesium cast and wrought components, without necessity of welding, was recently proposed (Papis, et al., 2010). The focus of this technique is on eliminating the natural oxide layer present on magnesium and replacing it with metallic Zn/MgZn₂ layer by a sequence of chemical, electrochemical and heat treatments. The objective is to change the surface reactivity and increase surface wettability to create Mg-Mg compound. The process verification, performed on AZ31 substrate, joined with AJ62 cast alloy and pure Mg, revealed an area-wide metallurgic in nature and defect free interface between both couples. The coating material dissolved into the bulk metal during casting. The issue of formation of shrinkage cavities at the interface can be solved by selecting appropriate solidification intervals (Fig. 10).

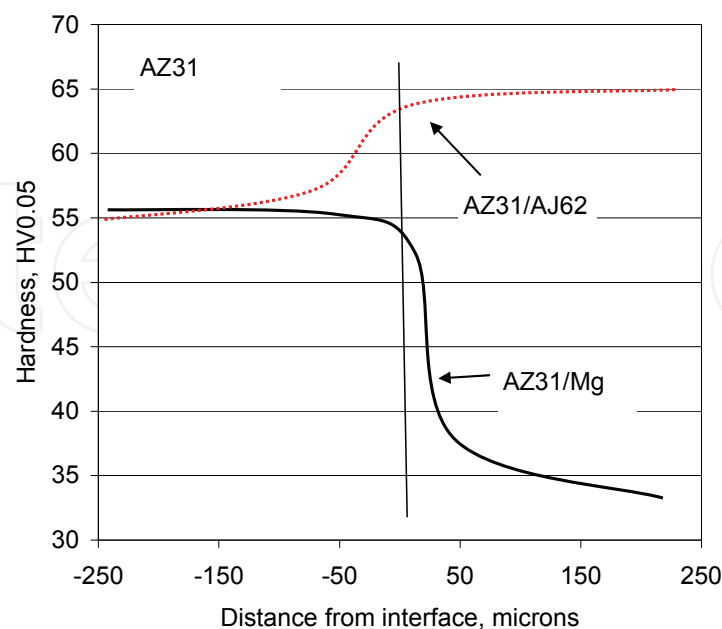


Fig. 10. Microhardness versus distance from interface for AZ31/AJ62 and AZ31/Mg connections using continuously metallurgic joining (Papis et al., 2010)

9. Other techniques of magnesium joining

This section describes joining techniques where diffusion is negligible or does not occur at all. Although no evident metallurgical bond is created, techniques satisfy many applications where other solutions are not viable due to technical or economical reasons.

9.1 Soldering

Soldering is a joining process where a filler metal with a melting temperature below 450 °C fills the joint by capillary action between closely fitting parts. Generally, magnesium is considered “unsolderable” by conventional means. There are, however, attempts to overcome this obstacle. Already in 1980’s, magnesium soldering flux, acetamid with a melting point of 82 °C, was developed which was able to dissolve magnesium oxide. As a solder, indium-tin with a melting point of 120 °C was proposed (Humpston and Jacobson, 2004).

Recently, high frequency induction soldering was found to be effective for joining magnesium alloy AZ31 (Ma et al., 2010). The process was conducted with a high frequency induction heating device using 80.8%Zn-19.2%Al filler metal and argon gas shielding. A wide temperature range and time of 120 s were applied. As a result of AZ31 alloy solution and transfer to soldering region, the solder chemistry changed during the process to 84.0%Zn-12.7%Al. In the soldering region, the α -Mg solid solution and α -Mg + Mg-Zn eutectoid were formed. The zinc solid solution and aluminum solid solution in the original filler metal disappeared completely. The joint achieved a shear strength of 19 MPa and fractured in the intercrystalline mode originating from the eutectoid structure.

There is a development in progress to find the suitable filler metals for magnesium. Several chemistries of Al-Zn-Mg alloys were proposed for soldering temperatures from 390 °C to 450 °C (Liu and Wu, 2010). For 25% of Al, range of Zn was of 25-95% and Mg of 2-72%. The role of Mg was to minimize a contact corrosion with the base metal, Zn due to the same crystal structure and electrode potential as Mg. The role of Al was to provide the joint strength. As a result, the Zn-enriched phases disappeared and α -Mg with dendritic morphology existed in the joint. The increased solidification rate by applying water cooling led to the formation of equiaxed fine dendrites and increasing their number by 40-50 times.

9.2 Brazing

Brazing is a joining process where a filler metal is placed at or between parts to be joined and the temperature is raised to melt the filler metal but not the work piece. The filler metal for brazing has the melting range above 450 °C.

Diffusion brazing methods are used to join advanced alloys and offer an alternative for dissimilar joints. A double stage process was applied to join stainless steel 316L to magnesium alloy AZ31 (Elthalabawy and Khan, 2010). In the first stage, thin nickel foil was diffusion bonded to stainless steel at 900 °C for 15 min and a pressure of 2 MPa. Then, the 316L/Ni was bonded in a vacuum chamber at 510 °C, a pressure 0.2 MPa and for time interval of 20 min. The possible phases between Ni and Mg may be deduced from Fig. 11.

A technique of brazing, called contact reaction brazing (CRB), is flux-free and benefits from low melting liquid phase formed by the eutectic reaction of dissimilar metals (Liu et al., 2008). A Zn interlayer with a thickness of up to 30 μ m provided solution in brazing of Mg with Al alloys. In particular case of AZ31 magnesium and A6061 aluminum alloys, the best shear strength was achieved by joints made with a 3 μ m thick Zn layer at 360 °C, 5 MPa

pressure and bonding times from 10 min to 30 min. Additions of Zn-based brazing alloy inhibited the formation of Mg-Al brittle phases. The Al substrate is bonded to the brazing alloy by a thin Al-Zn transition layer with no brittle phases. On the other side, the Mg plate is bonded to the brazing alloy by the reaction zone with low fraction of Mg-Zn intermetallics. At the interface between the reaction zone and the remnant brazing alloy, some pores were created, affecting a location of the failure zone (Liu et al., 2007b).

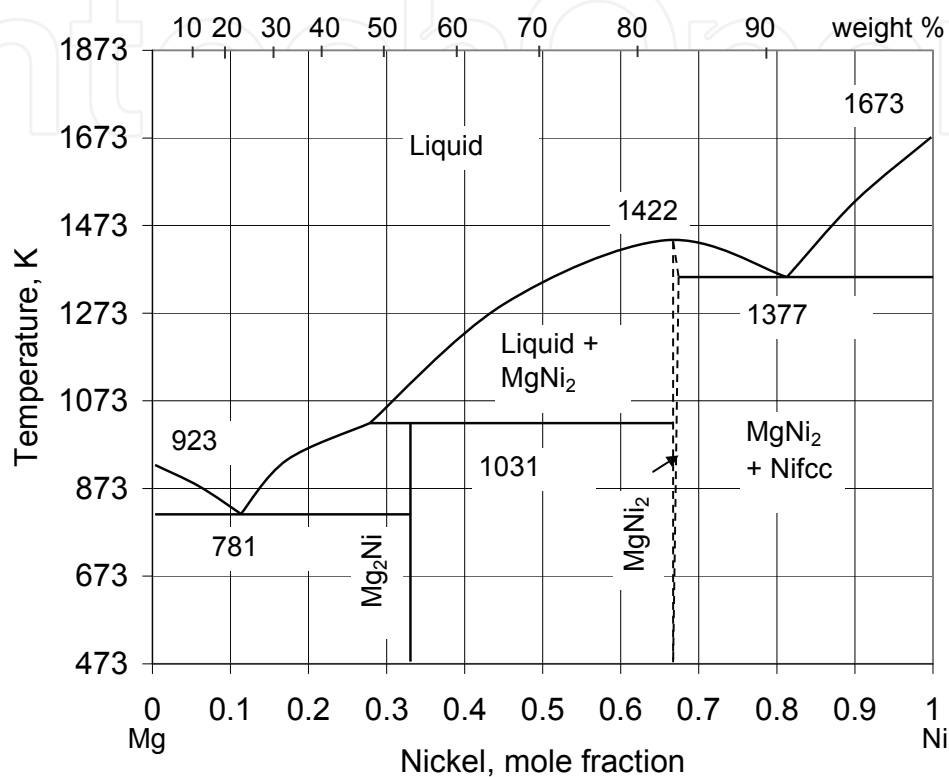


Fig. 11. Equilibrium phase diagram of Mg-Ni (Islam and Medraj, 2005; Zeng, 1999)

9.3 Adhesive bonding

Adhesive bonding is defined as joining using a non-metallic substance (adhesive) which undergoes hardening due to physical or chemical reaction. As a result, parts are joined together through surface adherence (adhesion) and internal strength (cohesion).

During adhesive bonding of magnesium alloys and polypropylene, satisfactory joint strength was achieved only after chemical pretreatment of both components (Liu and Xie, 2007b). An addition of 1% of SiO₂ particles into the adhesive increased the joint strength. The mechanism of bonding between polypropylene and the adhesive is based on diffusion and mechanical interaction. The bonding between magnesium alloy and adhesive is controlled by the coordinative bond forces.

10. Mechanical fastening of magnesium

10.1 Threaded fasteners

The galvanic corrosion of magnesium caused by fasteners is the key concern of mechanical joints. Although negligible corrosion occurs for 6000 series of aluminum alloys, for some applications the steel fasteners are required. A technique of Al plating of steel fasteners does

not present viable solution. A better compatibility in salt water environment exhibit steel fasteners with zinc or tin-zinc coatings, however they also experience corrosion due to the coating porosity. During performance simulation of mild steel fastener to AZ91 cast alloy in 5% NaCl solution, two corrosion mechanisms active in area from 1 to 2 cm from the interface were identified: galvanic corrosion and self corrosion (Jia et al., 2005). It was confirmed that the microgalvanic cells exist on the surface of AZ91D alloy which have potential differences of the order of 100 mV between alloy phases: matrix of α -Mg and $Mg_{17}Al_{12}$ intermetallics. This heterogeneous composition fuels both the galvanic and general corrosion. In addition to galvanic corrosion, steel fasteners have large difference in thermal expansion coefficient (Table 1) causing creep and preload loss if joint is subjected to thermal cycling, as is the case in an automotive engine.

Fasteners made of 6000 series of aluminum alloys, containing less than 1% of copper do not require additional surface treatment and their corrosion resistance does not change through their service life (Westphal et al., 2005). A comparison of clamp load of AlSi9Cu3 fasteners on AZ91 and AS21 cast alloys shows substantial lost of the preload after 200 h at 150 °C. At 120 °C the moderate lost of preload took place after 100 h of thermal exposure. At both temperatures there was no influence of magnesium alloy grade on the preload change.

10.2 Riveting

Riveting belongs to mechanical fastening methods which employs auxiliary joining elements. In self-piercing riveting the formation of holes, necessary in conventional process, is replaced by a combined cutting-riveting stage. Industrial applications include two processes based on half-hollow or solid type of rivets used. Self-piercing riveting is a high speed fastening for point joining of sheet materials with benefits shown in Fig. 12.

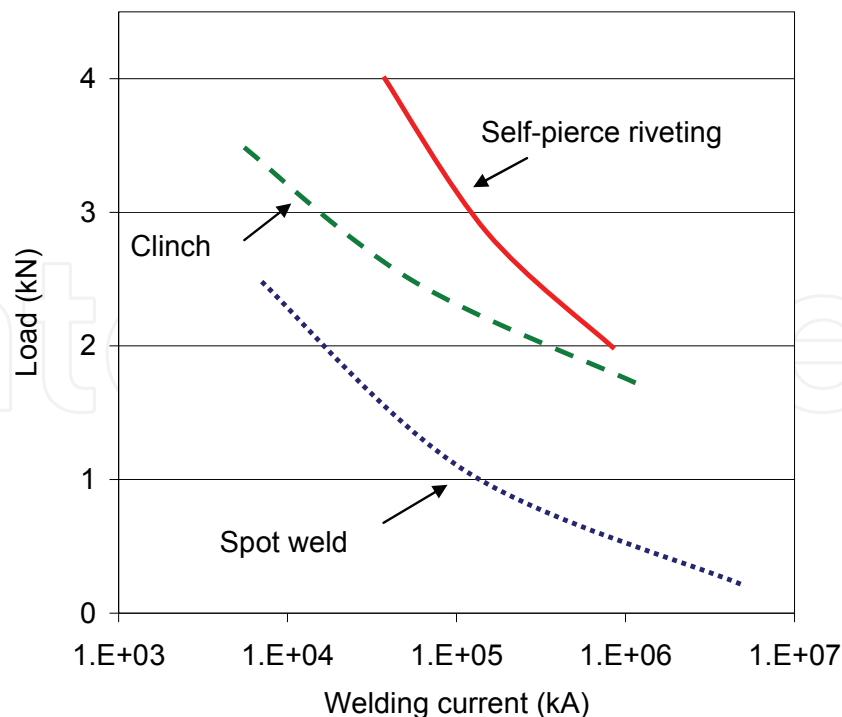


Fig. 12. Comparison of fatigue behaviour of joints obtained by spot-welding, clinching and self-pierce riveting (Cai et al., 2005)

A method of attaching a magnesium panel via self-piercing rivet was invented recently (Luo and Sachdev, 2010). The magnesium panel is spot heated and then the self-piercing steel rivet is punched through the steel panel and only partly through the magnesium panel, to displace the magnesium panel into the cavity. The purpose of heating is to improve formability of magnesium and prevent cracking. The invention proposes also solution to potential corrosion by concealing the interface between the steel rivet and the magnesium panel between the aluminum panel and magnesium panel. To prevent cracking, it is required to heat the magnesium panel in the region of the die cavity to a temperature of about 200 °C. The joint shows good combination of lap shear and cross-tension strength.

10.3 Clinching

Clinching represents a direct joining of materials using the forming technology where a local deformation of components with a rigid punch creates a form of locked joint. The wide variation of tools allows for a selection of the optimum joint geometry. Applicability of clinching for magnesium is limited by the low formability of magnesium at room temperature, causing cracking. To improve it, parts are heated up to 220 °C to increase an alloy formability. Two heating options are used in practice: heating of the entire part in a furnace or localized heating of the joint area using, for example, an induction method. Another option is to heat the die or punch to much higher temperature of almost 400 °C.

During conventional clinching the components are deformed together with a clinching punch in a contoured die, having a shape that controls the component interlocking. In a new solution, called dieless clinching, the contoured die is replaced by a flat anvil (Neugbauer et al., 2008). The benefit of the flat anvil as a counter tool is a possibility to decrease the heating time to 1 s instead of 3-6 s with the conventional clinching method. The heat is applied to the flat counter tool. A hybrid solution, combining clinching with adhesive bonding, was not successful since the adhesive layer was displaced during the first stage of clinching. Also experiments, combining a conventional clinching with contoured dies and adhesive bonding, cause problems due to inclusions of adhesive in the neck areas of the joint.

11. Summary

During last decade, a substantial progress was made in welding and joining of magnesium alloys. In addition to improvement in conventional fusion welding techniques, novel methods and their hybrids were developed. They allow producing commercially viable joints of different grades of cast and wrought magnesium alloys. Although there is a substantial progress on fusion welding, its application to dissimilar joints, which involve a number of materials with drastically different properties, is still limited. Also, alternative joining technologies, which require local deformation, are not fully successful due to limited formability of magnesium. To compensate low formability a preheating up to over 200 °C is required which diminishes the process economy. Low temperature processes, such as soldering and brazing, require improvement in joint strength by better control of interface phenomena. Novel ideas, aimed at eliminating the detrimental effect of natural oxides on magnesium surface seem to represent a step in correct direction. They may require complex surface engineering solutions but preliminary tests are promising. It is obvious, therefore, that there is a search for alternative methods of joining magnesium alloys, especially with dissimilar alloys.

12. References

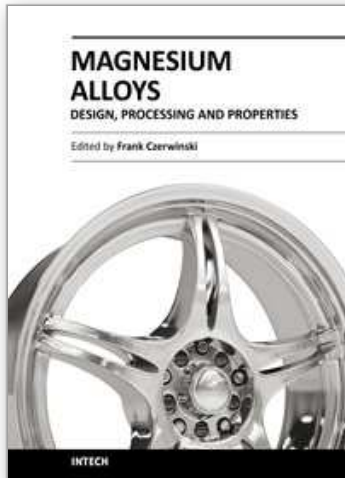
- Abderrazak, K., Salem, W. B., Mhiri, H., Lapalec, G. and Autric, M. (2008) Modeling of CeO₂ laser welding of magnesium alloys, *Optics and Laser Technology*, 40, 581-588
- Aizawa, T. and Kashani, M. (2010) Magnetic pulse welding (MPW) method for dissimilar sheet metal joints, *www.irjp.jp*,
- Aizawa, T., Kashani, M. and Okagawa, K. (2007) Application of magnetic pulse welding for aluminum alloys and SPCC steel sheet joints, *Welding Research*, 86, 119-124
- Al-Kazzaz, H., Medraj, M., Cao, X. and Jahazi, M. (2008) Nd:YAG laser welding of aerospace grade ZE41A magnesium alloy: Modeling and experimental investigations, *Materials Chemistry and Physics*, 109, 61-76
- ASM (1990) *Metals Handbook*, ASM International, Materials Park, Ohio
- Avedesian, M. M. (1999) *Magnesium and Magnesium Alloys*, ASM International, Materials Park, Ohio
- Barreiro, P., Schulze, V. and Loehe, D. (2008) Influence of process parameters on structure and mechanical properties of joints produced by electromagnetic forming and friction stir welding, *Advanced Materials Research*, 43, 47-56
- Cai, W., Wang, P. C. and Yang, W. (2005) Assembly dimensional prediction for self-piercing riveted aluminum panels, *Inter. Journal of Machine Tools Manufacturing*, 45, 695-704
- Chen, Y. C. and Nakata, K. (2009) Effect of tool geometry on microstructure and mechanical properties of friction stir lap welded magnesium alloy and steel, *Materials and Design*, 30, 3913-3919
- Chi, C., T., Chao, C. G., Liu, T. F. and Wang, C. C. (2008) Relational analysis between parameters and defects for electron beam welding of AZ-series of magnesium alloys, *Vacuum*, 82, 1177-1182
- Chi, C. T. and Chao, C. G. (2007) Characterization on electron beam welds and parameters for AZ31B-F extrusive plates, *Journal of Materials Processing Technology*, 182, 369-373
- Czerwinski, F. (2008) *Magnesium Injection Molding*, Springer Verlag, New York
- Elthalabawy, W. M. and Khan, T. I. (2010) Microstructural development of diffusion brazed austenitic stainless steel to magnesium using nickel interlayer, *Materials Characterization*, 61, 703-712
- Emam, S. A. and Domiaty, A. E. (2009) A refined energy-based model for friction-stir welding, *World Academy of Science, Engineering and Technology*, 53, 1016-1022
- Gilmore, C. J., Dunfold, D. V. and Parteidge, P. G. (1991) *Journal of Materials Science*, 26, 3119-3124
- Humpston, G. and Jacobson, D. M. (2004) *Principles of Soldering*, ASM International, Materials Park, Ohio
- Islam, F. and Medraj, M. (2005) The phase equilibria in the Mg-Ni-Ca system, *Calphad*, 29, 289-302.
- Jia, J. X., Atrens, A., Song, G. and Muster, T. H. (2005) Simulation of galvanic corrosion of magnesium coupled to a steel fastener in NaCl solution, *Materials and Corrosion*, 56, 7, 468-474

- Johnson, R. and Threadgill, P., Friction stir welding of magnesium alloys, *Magnesium Technology 2003*, 2003, TMS
- Kore, S. D., Imbert, J., Worswick, M. J. and Zhou, Y. (2009) Electromagnetic impact welding of Mg to Al sheets, *Science and Technology of Welding and Joining*, 14, 6, 549-553
- Kumbhar, N. T. and Bhanumurthy, K. (2008) Friction stir welding of Al6061 alloy, *Asian Journal of Experimental Science*, 22, 2, 63-74
- Lee, K. J., Kumai, S., Arai, T. and Aizawa, T. (2007) Interfacial microstructure and strength of steel/aluminum alloy lap joint fabricated by magnetic pressure seam welding, *Materials Science and Engineering A*, 471, 95-101
- Li, Y., Liu, P., Wang, J. and Ma, H. (2008) XRD and SEM analysis near the diffusion bonding interface of Mg/Al dissimilar materials, *Vacuum*, 82, 15-19
- Liu, L., Tan, J. and Liu, X. (2007b) Reactive brazing of Al alloy to Mg alloy using zinc-based brazing alloy, *Materials Letters*, 61, 2373-2377
- Liu, L., Wang, J. and Song, G. (2004) Hybrid laser-TIG welding, laser beam welding and gas tungsted arc welding of AZ31B magnesium alloy, *Materials Science and Engineering A*, 381, 129-133
- Liu, L. and Xie, L. (2007b) Adhesive bonding between Mg alloys and polypropylene, *Materials Technology: Advanced Performance Materials*, 22, 2, 76-80
- Liu, L. M., Tan, J. H., Zhao, L. M. and Liu, X. J. (2008) The relationship between microstructure and properties of Mg/Al brazed joints using Zn filler metal, *Materials Characterization*, 59, 479-483
- Liu, L. M., Wang, H. Y. and Zhang, Z. D. (2007a) The analysis of laser weld bonding of Al alloy to Mg alloy, *Scripta Materialia*, 56, 473-476
- Liu, L. M. and Wu, Z. (2010) Microstructure and interfacial reactions of soldering magnesium alloy AZ31B, *Materials Characterization*, 61, 1, 13-18
- Luo, A. A. and Sachdev, K. (2010) Method for attaching magnesium panels using self-piercing rivet, *US 2010/0083481*, April 8, 2010,
- Luo, Y., You, G., Ye, H. and Liu, J. (2010a) Simulation on welding thermal effect of AZ61 magnesium alloy based on three-dimensional modeling of vacuum electron beam welding heat source, *Vacuum*, 84, 890-895
- Ma, L., He, D. Y., Li, X. Y. and Jiang, J. M. (2010) High frequency soldering of magnesium alloy AZ31B using Zn-Al filler metal, *Materials Letters*, 64, 5, 596-598
- Mahendran, G., Balasuramanian, V. and Senthilvelan, T. (2010) Influence of diffusion bonding process parameters on bond characteristics of Mg-, *Transactions of Nonferrous Metals Society of China*, 20, 6, 997-1005
- Marya, M. and Edwards, G. R. (2002) Chloride contribution in flux-assisted GTA welding of magnesium alloys, *Welding Journal*, 12, 291-298
- Marya, M. and Edwards, G. R. (2000) The laser welding of magnesium alloy AZ91D, *Welding World*, 44, 2, 31-37
- Neugbauer, R., Kraus, C. and Dietrich, S. (2008) Advances in mechanical joining of magnesium, *CIRP Annals - Manufacturing Technology*, 57, 283-286
- Papis, K. J. M., Loffler, J. F. and Uggowitzer, P. J. (2010) Interface formation between liquid and solid Mg alloys - An approach to continuously metallurgic joining of magnesium parts, *Materials Science and Engineering A*, 527, 2274-2279

- Park, S. H. C., Sato, Y. S. and Kokawa, H. (2003) *Metallurgical and Materials Transactions A*, 34, 987
- Park, S. W. C., Sato, Y. S. and Kokawa, H. (2003a) Effect of micro-texture on fracture location in friction stir weld of Mg alloy AZ61 during tensile test, *Scripta Materialia*, 49, 161-166
- Poddar, D. (2009) Solid-state diffusion bonding of commercially pure titanium and precipitation hardening stainless steel, *International Journal of Recent Trends in Engineering*, 1, 5, 93-99
- Psyk, V., Beerwald, C., Klaus, A. and Kleiner, M. (2006) Characterization of extruded magnesium profiles for electromagnetic joining, *Journal of Materials Processing Technology*, 177, 266-269
- Quan, Y., Chen, Z., Yu, Z., Gong, X. and Li, M. (2008) Characteristics of laser welded wrought Mg-Al-Mn alloy, *Materials Characterization*, 59, 1799-1804
- Qui, X. and Song, G. (2010) Interfacial structure of the joints between magnesium alloy and mild steel with nickel as interlayer by hybrid laser-TIG welding, *Materials and Design*, 31, 605-609
- Shi, H., Qiu, R., Zhu, J., Zhang, K., Yu, H. and Ding, G. (2010) Effects of welding parameters on the characteristics of magnesium alloy joint welded by resistance spot welding with cover plates, *Materials and Design*, 31, 4853-4857
- Skar, J. I., Gjestland, H., Oosterkamp, L. and Albright, D. L., Friction stir welding of magnesium die castings, *Magnesium Technology 2004*, 2004, TMS, Warrendale
- Somekawa, H., Hosokawa, H., Watanabe, H. and Higashi, K. (2001) Experimental study of diffusion bonding in pure magnesium, *Materials Transactions*, 42, 10, 2075-2078
- Somekawa, H., Hosokawa, H., Watanabe, H. and Higashi, K. (2003a) Diffusion bonding in superplastic magnesium alloys, *Materials Science and Engineering A*, 339, 328-333
- Somekawa, H., Watanabe, H., Mukai, T. and Higashi, K. (2003b) Low temperature diffusion bonding in a superplastic AZ31 magnesium alloy, *Scripta Materialia*, 48, 1249-1254
- Sun, D. Q., Lang, B., Sun, D. X. and Li, J. B. (2007) Microstructure and mechanical properties of resistance spot welded magnesium alloy joints, *Materials Science and Engineering A*, 460, 461, 494-498
- Sun, D. X., Sun, D. Q., Gu, X. Y. and Xuan, Z. Z. (2008) Hot cracking of metal inert gas arc welded magnesium, *ISIJ International*, 49, 2, 270-274
- Wang, X. and Wang, K. (2006) Microstructure and properties of friction stir butt-welded AZ31 magnesium alloy, *Materials Science and Engineering A*, 431, 114-117
- Watanabe, T., Kagiya, K., Yanagisawa, W. and Tanabe, H. (2006) Solid state welding of steel and magnesium alloy using a rotating pin, *Quart. Journal of Japanese Welding Society*, 24, 108-123
- Westphal, K., Mulherkar, T. and Schneiding, W. (2005) Joining of magnesium components using Al fasteners, *Light Metal Age*, 4, 2-3

- Zeng, K. (1999) Thermodynamic analysis of the hydriding process of Mg-Ni alloys, *Journal of Alloys and Compounds*, 283, 213-224
- Zhao, H. and DebRoy, T. (2001) Pore formation during laser beam welding of die-cast magnesium alloy AM60B - mechanism and remedy, *Welding Research Supplement*, 8, 204-209
- Zhao, L. M. and Zhang, Z. D. (2008) Effect of Zn alloy interlayer on interface microstructure and strength of diffusion-bonded Mg-Al joints, *Scripta Materialia*, 58, 283-286
- Zhou, J., Li, L. and Liu, Z. (2005) CO₂ and diode laser welding of AZ31 magnesium alloy, *Applied Surface Science*, 247, 300-306

IntechOpen



Magnesium Alloys - Design, Processing and Properties

Edited by Frank Czerwinski

ISBN 978-953-307-520-4

Hard cover, 526 pages

Publisher InTech

Published online 14, January, 2011

Published in print edition January, 2011

Scientists and engineers for decades searched to utilize magnesium, known of its low density, for light-weighting in many industrial sectors. This book provides a broad review of recent global developments in theory and practice of modern magnesium alloys. It covers fundamental aspects of alloy strengthening, recrystallization, details of microstructure and a unique role of grain refinement. The theory is linked with elements of alloy design and specific properties, including fatigue and creep resistance. Also technologies of alloy formation and processing, such as sheet rolling, semi-solid forming, welding and joining are considered. An opportunity of creation the metal matrix composite based on magnesium matrix is described along with carbon nanotubes as an effective reinforcement. A mixture of science and technology makes this book very useful for professionals from academia and industry.

How to reference

In order to correctly reference this scholarly work, feel free to copy and paste the following:

Frank Czerwinski (2011). Welding and Joining of Magnesium Alloys, Magnesium Alloys - Design, Processing and Properties, Frank Czerwinski (Ed.), ISBN: 978-953-307-520-4, InTech, Available from: <http://www.intechopen.com/books/magnesium-alloys-design-processing-and-properties/welding-and-joining-of-magnesium-alloys>

INTECH
open science | open minds

InTech Europe

University Campus STeP Ri
Slavka Krautzeka 83/A
51000 Rijeka, Croatia
Phone: +385 (51) 770 447
Fax: +385 (51) 686 166
www.intechopen.com

InTech China

Unit 405, Office Block, Hotel Equatorial Shanghai
No.65, Yan An Road (West), Shanghai, 200040, China
中国上海市延安西路65号上海国际贵都大饭店办公楼405单元
Phone: +86-21-62489820
Fax: +86-21-62489821

© 2011 The Author(s). Licensee IntechOpen. This chapter is distributed under the terms of the [Creative Commons Attribution-NonCommercial-ShareAlike-3.0 License](#), which permits use, distribution and reproduction for non-commercial purposes, provided the original is properly cited and derivative works building on this content are distributed under the same license.

IntechOpen

IntechOpen